Available online at www.sciencedirect.com
SCIENCE DIRECT®
International Journal of Mass Spectrometry 242 (2005) 281–289
International Journal of Mass Spectrometry
www.elsevier.com/locate/ijms

Lead isotope ratio measurements in geological glasses by laser ablation-sector field-ICP mass spectrometry (LA-SF-ICPMS)

K.P. Jochum*, B. Stoll, K. Herwig, M. Amini[1], W. Abouchami, A.W. Hofmann

Max-Planck-Institut für Chemie, Postfach 3060, D-55020 Mainz, Germany

Received 23 September 2004; accepted 17 November 2004
Available online 12 January 2005

Abstract

We have tested the capabilities of LA-SF-ICPMS for in situ Pb isotopic work on geological glasses using a 213 nm Nd:YAG laser system and a double focusing magnetic sector field ICP mass spectrometer. Experiments were done with the MPI-DING and USGS reference glasses, USGS rock powders molten as glass beads and basaltic glasses from Hawaii. In particular, the precision and accuracy of $^{208}Pb/^{206}Pb$ and $^{207}Pb/^{206}Pb$ ratios were investigated for three-spot analyses of glasses with different Pb contents (0.4–40 μg/g) at spot sizes of 12–160 μm. Using the fast and precise electrical scan mode, we obtained for samples with Pb concentration >1 μg/g in-run precisions (1 R.S.E.) of better than 0.1% and 0.2% for spot diameters of 120 and 40 μm, respectively. The LA-SF-ICPMS isotope ratios agree with the high-precision TIMS and MC-ICPMS data within the external precision (R.S.D. = 0.1–0.2%). The LA-SF-ICPMS results for $^{208}Pb/^{204}Pb$, $^{207}Pb/^{204}Pb$ and $^{206}Pb/^{204}Pb$ are less precise (about 0.5–1%) due to the low abundance of ^{204}Pb and correction from the ^{204}Hg interference.

In this paper, we present the first LA-SF-ICPMS Pb isotope data for the MPI-DING (KL2-G, ATHO-G) and USGS reference glasses (BCR-2G, BHVO-2G) which may be useful for microanalytical in situ Pb isotope analysis. The findings of small (<2%), but significant differences in Pb isotope ratios of Hawaiian glasses of different ages, demonstrate that LA-SF-ICPMS is a suitable tool for geochemical research.

Keywords: LA-SF-ICPMS; Pb isotopes; MPI-DING reference glasses; USGS reference materials

1. Introduction

The determination of the abundances of the radiogenic Pb isotopes ^{208}Pb, ^{207}Pb and ^{206}Pb, daughter nuclides from ^{232}Th, ^{235}U and ^{238}U, respectively, in glass samples of oceanic basalts serves to investigate the chemistry and the evolution of the Earth's mantle. Microanalytical techniques, such as ion-microprobes [1,2] and more recently laser ablation-inductively coupled plasma-mass spectrometry (LA-ICPMS), have become important tools for in situ Pb isotope analysis. They have the advantage of high spatial resolution when compared with the conventional thermal ionization mass spectrometry (TIMS) technique, but suffer from lower precision and accuracy. In recent years, several authors [3–6] have shown that LA-ICPMS is suitable for in situ Pb geochronology of zircon using quadrupole-based and multi-collector (MC) instruments, respectively. Quadrupole instruments have the advantage of fast scan, but suffer from the lack of flat top peaks. LA-MC-ICPMS allows in situ determination of a wide variety of isotope ratios with internal precisions as low as ca. 10 ppm [7]. However, such high precisions have been achieved in samples with high elemental concentrations (>500 μg/g). The new generation of double-focusing magnetic sector field (SF) instruments is capable of very fast mass spectrum scans using both magnetic and electrical scan modes, has high sensitivity and flat peak tops. Recently, Tiepolo [8] demonstrated that the uncertainties on Pb isotope ratios in zircons using such mass spectrometers are in the 0.1–1.5% range.

* Corresponding author. Tel.: +49 6131 305216; fax: +49 6131 371051.
E-mail address: kpj@mpch-mainz.mpg.de (K.P. Jochum).
[1] Present address: Leibniz-Institut für Meereswissenschaften, IFM-GEOMAR, Wischofstr. 1-3, D-24148 Kiel, Germany.

1387-3806/$ – see front matter © 2004 Elsevier B.V. All rights reserved.
doi:10.1016/j.ijms.2004.11.019

The aim of this paper is to demonstrate that LA-SF-ICPMS with a 213 nm Nd:YAG laser can be used to determine Pb isotopes in geological glasses with Pb abundances as low as 0.4 μg/g with a precision and accuracy sufficient to interpret geological processes. For these investigations, we used geological reference glasses, a synthetic reference glass, reference materials molten to glass beads, and natural basaltic glasses from Hawaii. The concurrent determination of Pb isotope ratios using high-precision TIMS and MC-ICPMS allows to test the accuracy of the LA-SF-ICPMS technique.

2. Samples

The Max-Planck-Institut-Dingwell (MPI-DING) KL2-G and ATHO-G, the United States Geological Survey (USGS) BCR-2G and BHVO-2G, and the National Institute of Standards and Technology (NIST) SRM612 reference glasses were used for this investigation.

KL2-G and ATHO-G belong to the geological MPI-DING glasses that were prepared for providing reference materials for geochemical, in situ microanalytical work [9]. Large amounts (about 100 g) of reference glass were prepared by fusing the basalt KL2 from the Hawaiian volcano Kilauea and the rhyolite ATHO from Iceland, respectively. Reference values for more than 60 elements are published in Jochum et al. [9,10]. The determination of stable and radiogenic isotopes in the MPI-DING glasses is now in progress [10–13].

The USGS reference glasses have a basaltic composition. BCR-2G and BHVO-2G are fused glasses from rocks of the Columbia River Group and the Kilauea caldera. Elemental compositions are published in [14–16].

NIST SRM 612 is a synthetic reference glass commonly used as calibration material for trace element determinations in LA-ICPMS. Compilation data for more than 60 elements are listed in Pearce et al. [17]. Pb isotope data for this reference glass have been published by Woodhead and Hergt [18] and Baker et al. [26].

We also analyzed the USGS reference materials BCR-1, BCR-2, BHVO-1, BHVO-2, AGV-1, and AGV-2. In our laboratory, the rock powders were molten to glass beads by an electronically controlled iridium strip heater under Ar atmosphere, an equipment that is based on the design of Fedorowich et al. [19].

To demonstrate the potential application of direct Pb isotope measurements by LA-SF-ICPMS on natural glasses, we have analyzed handpicked ca. 200–500 μm × 100 μm glass fragments from the submarine section of the Hawaii Scientific Drilling Project (HSDP) [20]. These samples came from depths between 1300 and 3000 m below sea level.

3. Analytical technique

We used a New Wave UP-213 laser system combined with a single-collector double focusing magnetic sector ThermoFinnigan ICP mass spectrometer ELEMENT2. The laser system consists of a Q-switched Nd:YAG laser (213 nm wavelength) which was operated at 10 Hz. Ablation occurred in a He atmosphere. The He carrier gas was mixed with the Ar nebulizer gas flow prior to the plasma torch. Spot analyses were done using a typical spot diameter of 120 μm at an energy density of about 7 J/cm^2. To test the potential of LA-SF-ICPMS for microanalytical Pb isotopic work in geochemistry, some experiments were also performed using crater sizes varying between 12 and 160 μm. Ablation time varied between 10 and 120 s depending on the spot size, and the washout time between spots was 45 s. Blank count rates were measured for 20–50 s prior to ablation (Fig. 1).

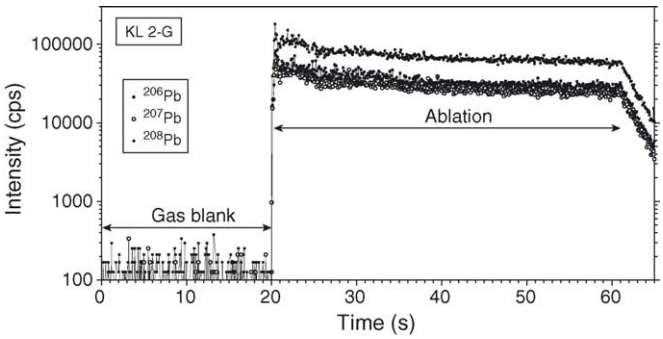

Fig. 1. Intensity of Pb isotopes measured during the spot analysis of KL2-G (Pb = 2.2 μg/g). The run consists of about 20 s blank and 40 s ablation measurements (120 μm spot diameter, 10 Hz). During spot analysis intensity decreases by less than 30%.

The ablated material was analyzed with an ELEMENT2 mass spectrometer equipped with the fast-scanning option. The low mass resolution mode with flat top peaks was used for this work. Experimental parameters were listed in Table 1. The mass spectrometer was tuned with NIST SRM612 so that the Pb sensitivity was high (about 50,000 cps/μg g^{-1} for ^{208}Pb using 120 μm spot size; Fig. 1). Typical background count rates were about 50 cps for Pb isotopes. Detection limit (3σ) for Pb was about 2 ng/g.

To measure the ^{206}Pb, ^{207}Pb and ^{208}Pb isotopes as precisely as possible, the electrical (Escan) mode was used. Measurements were done at a constant magnetic field by varying the accelerating and the electrostatic analyzer voltages. This scan is very fast; the time per pass varied from 0.075 s for the Pb mass scan, to 0.125 s for Pb and Tl mass range scan.

Table 1
Operating parameters

rf power	1270 W
Cool gas flow rate	15 L min^{-1}
Auxiliary gas flow rate	1.0 L min^{-1}
Carrier gas (Ar) flow rate	0.85 L min^{-1}
Carrier gas (He) flow rate	0.65 L min^{-1}
Sample time	0.002 s
Samples per peak	100
Mass window	10%
Counting mode	

Experiments were also performed using a combination of Escan and magnetic scan (Bscan) to measure simultaneously Pb isotopes and trace elements. In this mode, the magnet jumps to the first "magnet mass" and the predefined mass range will be scanned electrically. After this step, the magnet jumps to the next "magnet mass". Times per pass were typically 0.3–1 s. ^{43}Ca was the internal standard isotope for concentration measurements. ^{202}Hg was monitored to correct for the isobaric interference of ^{204}Hg (derived from the He gas) on ^{204}Pb. The precision and accuracy on ^{208}Pb/^{204}Pb, ^{207}Pb/^{204}Pb and ^{206}Pb/^{204}Pb ratios, especially for samples with low Pb contents (<1 μg/g), was poor due to the relatively high Hg blank.

Typically, a single Pb isotope value was obtained from three separate spot analyses, each of which consisted of about 250 blank and 500 ablation measurements using the Escan (Fig. 1) requiring 40 s of ablation time. In the combined Bscan–Escan mode, the number of ablation measurements was about 100 because of the much longer time per pass. Data reduction was done by calculating blank corrected Pb isotope ratios for each pass and by determining mean values of three runs. This procedure has the advantage to compensate the low (<30%) and steady intensity decrease during spot analysis (Fig. 1). At the beginning of the ablation (first 1–3 s), the Pb concentration was often found to be unusually high, mainly because of loosely consolidated material from previous ablation events that may deposit as a fine layer on the surface of the sample being analyzed. An outlier program rejected these values and other obvious outliers.

4. Precision and accuracy

The in-run precision (1 R.S.E.) depends mainly on the Pb concentration of the sample, the spot diameter and the scan mode used for analysis (Tables 2 and 3). Fig. 2 shows the influence of crater size and Pb concentration on the precision. For a three-spot analysis and a given Pb concentration of about 2 μg/g, the precision on the ^{208}Pb/^{206}Pb ratio (1 R.S.E.) obtained in Escan mode decreases from about 3%, at

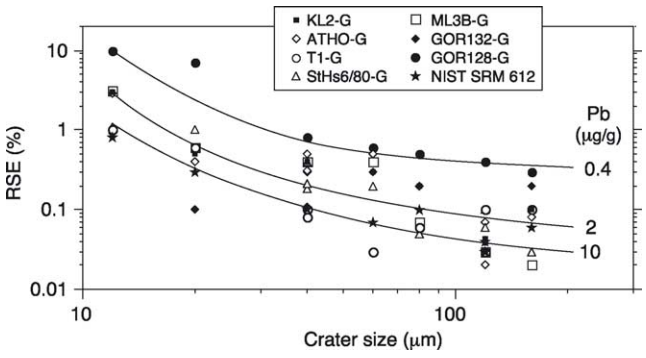

Fig. 2. Dependence of the in-run precision (1 relative standard error, R.S.E.) of ^{208}Pb/^{206}Pb ratio on the Pb concentration and the spot size used. Data are from three-spot analyses of MPI-DING and NIST glasses with different Pb contents.

Table 2
Pb isotope ratios of the MPI-DING reference glasses ATHO-G, KL2-G and the NIST SRM 612 glass obtained from three-spot LA-SF-ICPMS analyses using different spot sizes and the Escan mode of the mass spectrometer

Analysis	1	2	3	4	5	6	7	8	9	10	11	12	13	Mean (analysis 10–13)	R.S.D. (%)	Reference values	Dev. (%)
Spot size (μm)	12	20	40	40	40	40	40	60	80	120	120	120	160	120–160 μm			
^{208}Pb/^{206}Pb																	
NIST SRM 612	2.120	2.178	2.153	2.161	2.167		2.154	2.162	2.153		2.156	2.162	2.152	2.157	0.2	2.165	−0.4
R.S.E. (%)	1	0.3	0.4	0.2	0.1		0.3	0.07	0.1		0.03	0.04	0.06				
ATHO-G	2.100	2.100	2.078	2.075	2.072	2.065	2.093	2.072	2.077	2.072	2.073	2.073	2.073	2.073	0.09	2.0729	−0.01
R.S.E. (%)	7	0.4	0.4	0.3	0.3	0.3	0.5	0.5	0.2	0.04	0.02	0.07	0.08				
KL2-G	2.020	2.030	2.028	2.025	2.018	2.026	2.034	2.021	2.026	2.023	2.023	2.025	2.026	2.024	0.07	2.0244	−0.01
R.S.E. (%)	3	0.5	0.4	0.3	0.4	1	0.4	0.3	0.2	0.03	0.04	0.04	0.1				
^{207}Pb/^{206}Pb																	
NIST SRM 612	0.9070	0.9079	0.9053	0.9077	0.9086		0.9056	0.9062	0.9091		0.9110	0.9092	0.9098	0.9100	0.1	0.9074	0.3
R.S.E. (%)	3	0.3	0.5	0.3	0.1		0.2	0.09	0.09		0.1	0.1	0.05				
ATHO-G	0.8010	0.8520	0.8480	0.8446	0.8358	0.8379	0.8485	0.8399	0.8418	0.8414	0.8424	0.8392	0.8439	0.8417	0.2	0.84201	−0.03
R.S.E. (%)	2	1	1	0.7	0.2	0.4	0.06	0.3	0.09	0.1	0.1	0.03	0.1				
KL2-G	0.7800	0.8260	0.8293	0.8221	0.8172	0.8167	0.8221	0.8129	0.8217	0.8225	0.8226	0.8225	0.8224	0.8225	0.04	0.82147	0.1
R.S.E. (%)	3	1	0.5	0.8	1	0.3	0.5	0.80	0.2	0.02	0.3	0.1	0.1				

Pb concentrations are: ATHO-G: 5.7 μg/g; KL2-G: 2.2 μg/g [9]; NIST SRM 612:39.0 μg/g [17]. Reference values for MPI-DING glasses are mean of TIMS (analysts: J. Pfänder, M. Amini, W. Abouchami) and MC-ICPMS (J. D. Woodhead) data [10]; NIST SRM 612 reference values are from [18,26]. Dev.: deviation of LA-SF-ICPMS data from the reference values.

Table 3
Pb isotope ratios of the MPI-DING reference glasses ATHO-G, KL2-G and the NIST SRM 612 glass obtained from three-spot LA-SF-ICPMS analyses using spot sizes of 40 and 120 μm and the combined Bscan–Escan mode

Analysis	1	2	3	4	5	6	7	8	9	10	11	Mean (analysis 3–11)	R.S.D. (%)	Reference values	Dev. (%)
Spot size (μm)	40	40	120	120	120	120	120	120	120	120	120	120 μm			
$^{208}Pb/^{206}Pb$															
NIST SRM 612	2.151	2.154	2.152	2.179	2.171	2.168	2.157	2.148	2.141	2.141	2.154	2.157	0.6	2.165	−0.4
R.S.E. (%)	0.3	1	1	1	0.6	0.3	0.2	0.6	0.2	0.4	0.2				
ATHO-G	2.073	2.063	2.073	2.081	2.080	2.073	2.071	2.079	2.078	2.069	2.074	2.075	0.2	2.0729	0.1
R.S.E. (%)	0.5	0.6	0.02	0.1	0.2	0.7	0.3	0.2	0.7	0.1	0.3				
KL2-G	2.019	2.028	2.028	2.013	2.027	2.037	2.016	2.014	2.012	2.012	2.027	2.021	0.5	2.0244	−0.2
R.S.E. (%)	0.4	0.8	0.1	0.1	0.05	0.3	0.2	0.7	0.2	0.3	0.3				
$^{207}Pb/^{206}Pb$															
NIST SRM 612	0.9063	0.9052	0.9032	0.9110	0.9151	0.9107	0.9113	0.9056	0.9090	0.9045	0.9088	0.9088	0.4	0.9074	0.2
R.S.E. (%)	0.5	0.9	0.8	0.3	0.4	0.5	0.2	0.9	0.1	0.2	0.4				
ATHO-G	0.8432	0.8450	0.8450	0.8405	0.8438	0.8402	0.8477	0.8454	0.8460	0.8419	0.8469	0.8442	0.3	0.84201	0.3
R.S.E. (%)	0.3	0.8	0.5	0.6	0.01	0.4	0.4	0.4	0.1	0.1	0.5				
KL2-G	0.8282	0.8285	0.8255	0.8250	0.8192	0.8243	0.8197	0.8237	0.8205	0.8218	0.8128	0.8214	0.5	0.82147	0.0
R.S.E. (%)	0.4	0.3	0.05	0.5	0.2	0.3	0.9	0.3	0.5	0.3	0.8				
$^{208}Pb/^{204}Pb$															
NIST SRM 612	37.21	37.08	37.11	37.47	37.29	36.82	36.81	37.03	36.07	36.28	36.89	36.86	1.2	37.010	−0.4
R.S.E. (%)	1.4	2.2	0.6	1.3	1.2	0.6	0.3	0.9	0.8	0.4	0.3				
ATHO-G	37.86	39.01	38.84	38.75	38.86	39.16	38.07	39.88	38.48	37.98	39.24	38.81	1.5	38.101	1.9
R.S.E. (%)	2.5	1.8	0.5	0.6	0.5	2	0.5	2	3	0.5	1				
KL2-G	37.42	38.43	38.86	38.85	38.95	40.21	37.94	36.31	37.41	39.01	39.99	38.61	3.2	38.524	0.2
R.S.E. (%)	4.1	0.7	0.8	0.6	1	1	0.3	4	0.3	0.9	1				
$^{207}Pb/^{204}Pb$															
NIST SRM 612	15.75	15.68	15.62	15.61	15.70	15.47	15.58	15.68	15.55	15.34	15.59	15.57	0.7	15.51	0.4
R.S.E. (%)	0.5	2.8	3	0.2	1	0.6	0.3	1	0.7	0.3	0.3				
ATHO-G	15.49	15.97	15.80	15.64	15.75	15.93	15.55	16.41	15.69	15.46	16.04	15.81	1.8	15.477	2.1
R.S.E. (%)	3	3	0.7	0.2	0.03	2	0.5	2	2	0.5	1				
KL2-G	15.87	15.65	15.83	15.91	15.78	16.18	15.48	15.13	15.36	15.93	16.44	15.78	2.6	15.633	1.0
R.S.E. (%)	5.6	1.3	0.1	1	0.9	0.7	0.3	3	0.2	1	1				
$^{206}Pb/^{204}Pb$															
NIST SRM 612	17.77	17.39	17.42	17.15	17.01	16.98	17.10	17.41	17.22	16.96	17.17	17.16	1.0	17.097	0.4
R.S.E. (%)	2	2	2	0.5	0.5	0.2	0.2	0.8	0.9	0.1	0.2				
ATHO-G	18.38	19.33	18.64	18.58	18.66	19.07	18.35	19.52	18.53	18.33	19.02	18.74	2.1	18.381	2.0
R.S.E. (%)	4	2	0.4	0.7	0.2	2.0	0.4	2	2	0.5	1				
KL2-G	19.21	19.33	19.13	19.37	19.21	19.63	19.05	18.44	18.75	19.46	19.78	19.20	2.2	19.030	0.9
R.S.E. (%)	2	2	0.2	0.8	1	1	1	2	0.5	0.8	1				

Reference values: see Table 2. Dev.: deviation of LA-SF-ICPMS data from the reference values.

very small crater sizes of 12 μm (corresponding crater depths 10–20 μm), to values of <0.1% at crater sizes ≥80 μm (crater depths = 80–100 μm). An in-run precision of about 0.05% was reached for larger spot sizes of 120 and 160 μm.

$^{208}Pb/^{206}Pb$ ratios can also be determined in samples with Pb concentrations as low as 0.4 μg/g, however, with a factor of four lower precision independent of the spot size. For higher Pb concentrations (>2 μg/g), the precision improves significantly. The in-run precision of the $^{207}Pb/^{206}Pb$ measurements is similar to that of $^{208}Pb/^{206}Pb$ as shown in Fig. 2.

The precision of LA-SF-ICPMS data in Escan mode is similar to that obtained by secondary ionization mass spectrometry (SIMS) using a Cameca IMS 1270 ion-microprobe. Saal et al. [2], using SIMS, showed that the in-run precision correlates with the Pb content of the sample; typical in-run precision (1 R.S.E.) for Pb isotopic measurements ($^{208}Pb/^{206}Pb$ and $^{207}Pb/^{206}Pb$) ranged from about 0.1% (^{208}Pb count rates = 10,000 cps) to 0.6% (^{208}Pb count rates = 200 cps) for a spot diameter of 20–30 μm and typical ^{208}Pb count rates of 400 cps/μg/g total Pb. This means that the in-run precision for $^{208}Pb/^{206}Pb$ SIMS measurement of a glass having a total Pb content of about 2 μg/g is about 0.5%. Our LA-SF-ICPMS data (Fig. 2) indicate that the R.S.E. of a three-spot analysis is about 0.2% (corresponding to about 0.4% for a single spot analysis) for 2 μg/g Pb samples and 40 μm spot size. This comparison indicates that both SIMS and LA-SF-ICPMS methods yield similar precision.

$^{208}Pb/^{206}Pb$ and $^{207}Pb/^{206}Pb$ data of the combined Bscan–Escan mode (Table 3) are about a factor of 2–4 less precise than the Escan mode (Fig. 3). This is due to the longer time per pass required which results in a decrease of the number of Pb measurements for a three-spot analysis (about 3× 100 compared to 3× 500) and an increase of ion beam instabilities. The precision on the $^{208}Pb/^{204}Pb$, $^{207}Pb/^{204}Pb$ and $^{206}Pb/^{204}Pb$ ratios is even lower because of the low abundance of ^{204}Pb and errors induced from the ^{204}Hg interference correction on this isotope. In SIMS [2], the in-run precision for $^{208}Pb/^{204}Pb$, $^{207}Pb/^{204}Pb$ and $^{206}Pb/^{204}Pb$ is similar to our LA-SF-ICPMS data ranging from 0.3 (10,000 cps for ^{208}Pb) to 0.8% (2000 cps for ^{208}Pb).

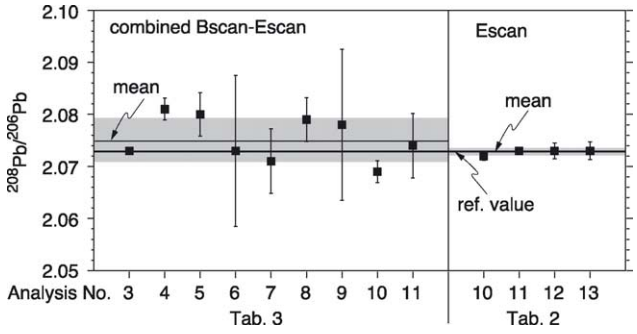

Fig. 3. $^{208}Pb/^{206}Pb$ ratios obtained from different analyses using spot sizes ≥120 μm by combined Bscan–Escan and Escan modes. Error bars correspond to ± 1 S.E. The shaded bands represent the external precision (±1 S.D.). Reference value used is from high-precision TIMS and MC-ICPMS analyses.

Mass fractionation (MF) is another important source of error in isotope measurements. The measured isotope ratios differ from the true value due to fractionation processes that are mass dependent, such as instrumental mass discrimination, laser ablation induced fractionation and energy dependent detector efficiency. For the accurate determination of the Pb isotope ratios by LA-SF-ICPMS, a linear function was sufficient to correct MF. MF was calculated by

$$\mathrm{MF} = \left(\frac{(A_i/A_k)_{\mathrm{true}}}{(A_i/A_k)_{\mathrm{meas}}} - 1\right) \times \left(\frac{1}{\Delta m_{A_i - A_k}}\right)$$

where $(A_i/A_k)_{\mathrm{true}}$ and $(A_i/A_k)_{\mathrm{meas}}$ are the true and the measured intensity ratios between the isotopes i and k and $\Delta m_{A_i - A_k}$ is the mass difference (Da) between i and k.

MF was determined from the deviation of the measured $^{205}Tl/^{203}Tl$ ratio in the NIST SRM 612 from the literature value of 2.3871 ± 0.0013 [21]. The Tl concentration (15.07 μg/g [17]) in the reference glass is high enough to obtain precise $^{205}Tl/^{203}Tl$ results by LA-SF-ICPMS (R.S.E. of <0.1% for crater sizes ≥40 μm). MF values were constant during several hours; however, they varied from experiment to experiment. This is shown in Fig. 4 where the deviations of the LA-SF-ICPMS $^{208}Pb/^{206}Pb$ ratios of the MPI-DING glasses ATHO-G and KL2-G from the high precision TIMS and MC-ICPMS values (Table 2) are plotted versus the deviation of our measured $^{205}Tl/^{203}Tl$ from the accepted literature value. The correlations indicate the validity of this external calibration procedure, using Tl ratios measured in NIST SRM 612. MF varied between −0.5 and 0.5 % Da^{-1} for the different experiments using 60–160 μm laser craters. The uncertainty on MF using the Tl isotope composition of NIST SRM 612 is about 0.08% (1 S.D.) (see Fig. 4). This error takes into account possible $^{205}Tl/^{203}Tl$ variations in the NIST glass [26] from a natural, constant ratio of 2.3871 as assumed in this study.

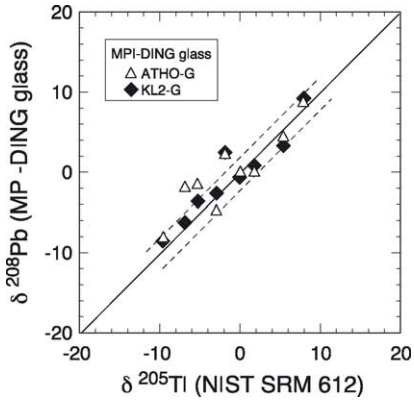

Fig. 4. Correlation of mass fractionation for Pb isotopes (determined in two MPI-DING glasses) with Tl isotopes (determined in NIST SRM 612). Data are from Escan analyses with spot sizes 60–160 μm. Reference values for $^{208}Pb/^{206}Pb$ ratios are from TIMS and MC-ICPMS analyses (Table 2); $(^{205}Tl/^{203}Tl)_{\mathrm{lit}} = 2.3871$ [21]. Uncertainty of mass fractionation correction is ±0.08% as shown by dashed lines: $\delta^{205}Tl = ((^{205}Tl/^{203}Tl)_{\mathrm{meas}}/(^{205}Tl/^{203}Tl)_{\mathrm{lit}} - 1) \times 1000$ and $\delta^{208}Pb = ((^{208}Pb/^{206}Pb)_{\mathrm{meas}}/(^{208}Pb/^{206}Pb)_{\mathrm{ref}} - 1) \times 1000$.

The overall analytical uncertainty on Pb isotope ratios includes the in-run precision and correction uncertainties related to mass fractionation. The in-run precision on the $^{208}Pb/^{206}Pb$ and $^{207}Pb/^{206}Pb$ ratios is <0.1% for Pb concentrations >1 μg/g using a three-spot analysis in Escan mode with spot diameters ≥120 μm. This means that the uncertainty on the external mass fractionation correction (about 0.08%) is similar to or even higher than the in-run precision. The overall analytical uncertainty is therefore <0.18% for Pb >1 μg/g samples. For lower Pb contents (0.4–1 μg/g), the smaller spot sizes used (40–80 μm) and/or the use of the combined Bscan–Escan mode result in an overall higher analytical uncertainty of about 0.2–1%.

The overall analytical uncertainty is similar to the reproducibility (external precision) which is based on the results of different independent analyses. Table 2 and Fig. 3 show that the external precision (1 R.S.D.) is about 0.1–0.2% for $^{208}Pb/^{206}Pb$ and $^{207}Pb/^{206}Pb$ in KL2-G and ATHO-G using spot sizes of 120–160 μm and Escan mode.

5. Results and discussion

Minimum spot size, precision and accuracy of the data are the most important parameters for testing the capabilities of LA-SF-ICPMS for in situ Pb isotopic work of geological glasses. Fig. 5 shows the $^{208}Pb/^{206}Pb$ ratios with the corresponding standard errors (S.E.) for ATHO-G and KL2-G using crater sizes of 12, 20, 40, 60, 80, 120 and 160 μm, respectively. As already shown in Fig. 2, the analytical error decreases with increasing crater sizes. New reference values obtained from high-precision TIMS and MC-ICPMS analyses (Table 2) show that the $^{208}Pb/^{206}Pb$ ratio for ATHO-G is significantly higher than that of KL-2G. This is also confirmed by our LA-SF-ICPMS results. With the exception of the 12 μm measurements, the differences are clearly resolved. Nearly all ratios agree within ± 1 S.E. with the reference values. Especially promising is the low error on $^{208}Pb/^{206}Pb$ ratio and the good agreement with the high-precision TIMS and MC-ICPMS data for spot sizes ≥120 μm. Therefore, only Pb isotope data from analyses with spot diameters ≥120 μm have been used to characterize the samples. Tables 2, 4 and 5 report the results of the more precise Escan analyses, whereas Table 3 presents all Pb isotope data obtained by the combined Bscan–Escan mode. Pb concentrations are also listed. The mean $^{208}Pb/^{206}Pb$ and $^{207}Pb/^{206}Pb$ values of 4–5 independent LA-ICPMS analyses of KL2-G and ATHO-G are identical within 0–0.1% with the reference values (Table 2). These deviations are similar to external precision of the LA-SF-ICPMS data (0.1–0.2%) indicating that sample heterogeneity and calibration errors are small. Tables 2 and 3 contain the first Pb isotope data for the MPI-DING glasses KL2-G

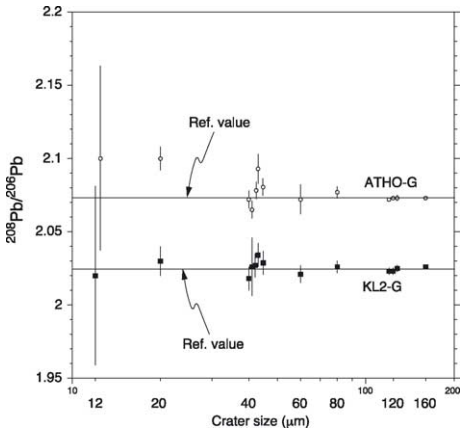

Fig. 5. $^{208}Pb/^{206}Pb$ ratios obtained from sets of three-spot analyses using different spot sizes. Error bars indicate ± 1 S.E. ($N = 3$). The data are compared with reference values from TIMS and MC-ICPMS analyses.

Table 4
Pb isotope ratios of USGS reference materials obtained from three-spot analyses using a spot size of 120 μm and the Escan mode of the mass spectrometer

USGS reference material	$^{208}Pb/^{206}Pb$			$^{207}Pb/^{206}Pb$			Pb (μg/g)
	LA-SF-ICPMS	Reference values	Dev. (%)	LA-SF-ICPMS	Reference values	Dev. (%)	
AGV-1	2.036	2.0358	0.01	0.8284	0.8266	0.2	36
R.S.E. (%)	0.05			0.1			
AGV-2	2.049	2.0421	0.3	0.8295	0.8276	0.2	13.4
R.S.E. (%)	0.1			0.3			
BCR-1	2.061	2.0577	0.2	0.8311	0.8308	0.04	13.6
R.S.E. (%)	0.1			0.1			
BCR-2	2.064	2.0643	−0.01	0.8333	0.8328	0.06	11.5
R.S.E. (%)	0.04			0.09			
BCR-2G	2.062			0.8333			10.8
R.S.E. (%)	0.06			0.1			
BHVO-1	2.051	2.052	−0.05	0.8342	0.8331	0.1	2.6
R.S.E. (%)	0.2			0.6			
BHVO-2	2.051	2.051	0.00	0.8339	0.8336	0.04	1.9
R.S.E. (%)	0.1			0.08			
BHVO-2G	2.050			0.8331			1.8
R.S.E. (%)	0.1			0.2			

Reference values are from [22,26]. Pb concentrations are mean values from [25] and the MPI-Mainz database for reference materials. Dev.: deviation of LA-SF-ICPMS data from the reference values.

Table 5
Pb isotope ratios of handpicked glass fragments of HSDP samples obtained from three-spot analyses using a spot size of 120 μm and the Escan mode of the mass spectrometer

HSDP glasses	$^{208}Pb/^{206}Pb$			$^{207}Pb/^{206}Pb$			Pb (μg/g)
	LA-SF-ICPMS	TIMS	Dev. (%)	LA-SF-ICPMS	TIMS	Dev. (%)	
SR 515-3.6 G	2.058	2.0606	−0.1	0.8366	0.83725	−0.08	0.78
R.S.E. (%)	0.04	0.002		0.3	0.002		
SR 542-9.6 G	2.062	2.0670	−0.2	0.8363	0.83932	−0.4	0.87
R.S.E. (%)	0.3	0.003		0.2	0.002		
SR 759-4.0 G	2.075			0.8410			
R.S.E. (%)	0.1			0.3			
SR 764-11.5 G	2.082	2.0702	0.6	0.8470	0.83926	0.9	0.83
R.S.E. (%)	0.2	0.002		0.4	0.001		
SR 889-13.6 G	2.052	2.0557	−0.2	0.8303	0.83400	−0.4	0.67
R.S.E. (%)	0.3	0.002		0.3	0.002		
SR 912-18.0 G	2.048	2.0501	−0.1	0.8286	0.83128	−0.3	0.79
R.S.E. (%)	0.3	0.002		0.2	0.002		
SR 942-5.7 G	2.058	2.0628	−0.2	0.8361	0.83804	−0.2	0.65
R.S.E. (%)	0.5	0.003		0.5	0.002		
SR 961-14.0 G	2.066	2.0611	0.2	0.8368	0.83717	−0.04	1.5
R.S.E. (%)	0.2	0.002		0.2	0.001		

Pb concentration data by LA-SF-ICPMS (MPI-Mainz). Dev.: deviation of LA-SF-ICPMS data from the TIMS values.

and ATHO-G. These values should be useful to practitioners of microanalytical techniques to calibrate their isotope measurements. Our $^{208}Pb/^{206}Pb$ and $^{207}Pb/^{206}Pb$ measurements for NIST SRM 612 are 0.4% lower and about 0.3% higher, respectively, than the published values [18]. Possible reasons for these discrepancies are a worse ablation behavior of the transparent NIST glass, and measuring problems using counting mode for high Pb concentration and sample heterogeneities.

Although the Bscan–Escan combined mode yield less precise data (Table 3), the results agree with the reference values. External precision is 0.2–0.5% for $^{208}Pb/^{206}Pb$ and $^{207}Pb/^{206}Pb$. For $^{208}Pb/^{204}Pb$, $^{207}Pb/^{204}Pb$ and $^{206}Pb/^{204}Pb$ ratios, the reproducibilities and deviations are much higher (0.2–3%).

The USGS reference materials AGV-1, AGV-2, BCR-1, BCR-2, BHVO-1 and BHVO-2 were analyzed as quenched glasses (Table 4). Most values agree with published TIMS data. Woodhead and Hergt [22] and Baker et al. [26] found small, but significant differences in Pb isotopic composition ($^{208}Pb/^{204}Pb$, $^{207}Pb/^{204}Pb$, $^{206}Pb/^{204}Pb$) between the new (BCR-2, BHVO-2, AGV-2) and the original (BCR-1, BHVO-1, AGV-1) samples. Fig. 6 shows a comparison of the TIMS and LA-SF-ICPMS data. Differences in the $^{208}Pb/^{206}Pb$ and $^{207}Pb/^{206}Pb$ ratios obtained by LA-SF-ICPMS can be detected, although some may not be significant due to the larger errors. The Pb isotope data for the USGS reference glasses BCR-2G and BHVO-2G are similar to the powdered, original reference materials BCR-2, BHVO-2. So far, no published Pb isotope measurements for these samples exist.

The LA-SF-ICPMS technique has also been applied for the analysis of natural glass fragments recovered from the Hawaiian Scientific Drill Hole (HSDP-2) through Mauna Kea volcano (Fig. 7). Table 5 and Fig. 8 report the LA-SF-ICPMS data of eight samples from different depths in the drill core. Significant differences are found in the $^{208}Pb/^{206}Pb$ ratios stratigraphy and are consistent with the temporal Pb isotope variations found in the HSDP-2 core based on the whole-rock TIMS Pb isotope data [23] obtained using the triple spike method [24].

Table 5 also lists the TIMS Pb triple spike data obtained on the HSDP-2 glasses in our laboratory. For the TIMS measurements, 50 mg of the glass fragments were used, in contrast with the 10 μg size sample required for the LA-SF-ICPMS. With the exception of sample SR 764, the LA-SF-ICPMS data agree with the triple spike data within error limits. Fig. 8 shows that both datasets lie on the same trend with no systematic offset. The possible reason for the difference between TIMS and LA-SF-ICPMS values found in sample SR 764 is that palagonite (altered glass) and inclusions in the sample were identified and discarded for the LA-SF-ICPMS measurement, while they may have not been entirely removed by

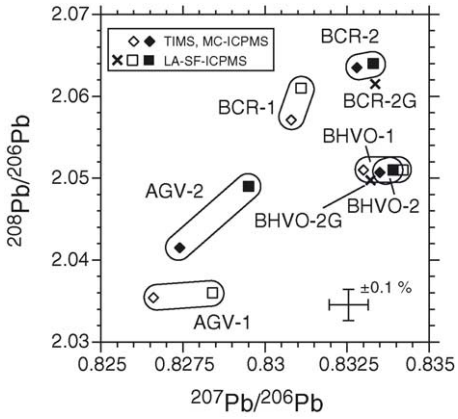

Fig. 6. $^{208}Pb/^{206}Pb$ vs. $^{207}Pb/^{206}Pb$ for USGS reference materials. TIMS [22], MC-ICPMS [26] and LA-SF-ICPMS (Table 4) results of the same materials are indicated by envelopes.

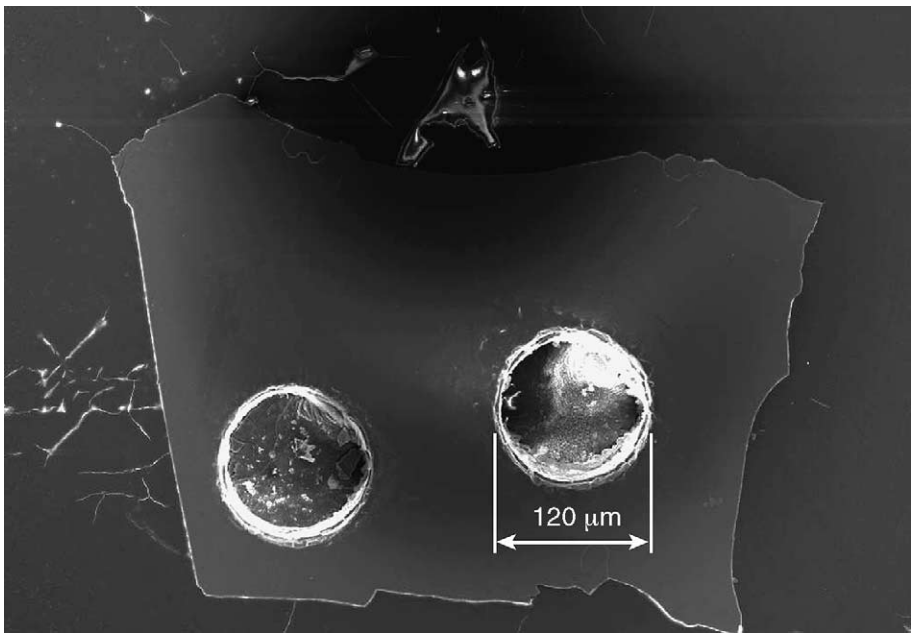

Fig. 7. Laser craters (120 μm diameter) drilled with a 213 nm Nd:YAG laser (ablation time = 60 s) in a glass fragment of a Hawaiian basalt from the HSDP-2 drill core.

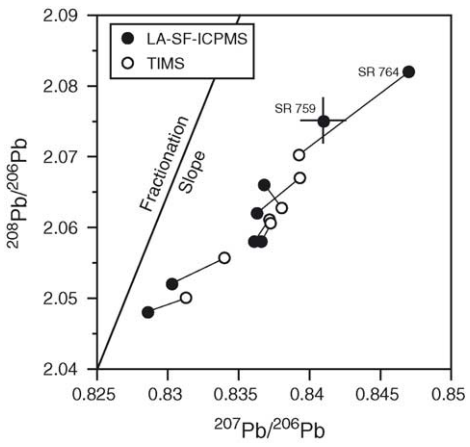

Fig. 8. Comparison of Pb isotope data obtained by LA-SF-ICPMS with high precision TIMS data for HSDP-2 glasses. Note the good agreement between the two data sets within analytical uncertainties.

the mild leaching used for the TIMS analyses (cold HCl 1N). Another reason may be sample heterogeneity.

6. Conclusions

Our experiments on homogeneous glasses show that LA-SF-ICPMS using a 213 nm Nd:YAG laser and a sector field ICP mass spectrometer is a suitable and very fast technique for in situ Pb isotope analysis. Reproducibilities of better than 0.1% are achieved for spot sizes ≥120 μm in samples with Pb contents in the μg/g range. Even for spot sizes of 40 μm, we obtain reproducibilities of 0.3%. Our external correction for mass-dependant fractionation using Tl isotopes leads to a good agreement with high-precision TIMS and MC-ICPMS data. The sensitivity and precision of this method is comparable to that obtained by SIMS methods using the Cameca IMS 1270 ion probe. Our results demonstrate that LA-SF-ICPMS can be applied as microanalytical tool for Pb isotope ratio measurements in a variety of geological samples, such as melt inclusions, minerals and natural glasses.

Acknowledgements

We thank J. Pfänder and J.D. Woodhead for providing analytical data of the MPI-DING reference glasses.

References

[1] I.S. Williams, in: M.A. McKibben, W.C. Shanks, W.I. Ridley (Eds.), Application of Microanalytical Techniques to Understanding Mineralizing Processes. Reviews in Economic Geology, vol. 7, 1998, p. 126.
[2] A.E. Saal, S.R. Hart, N. Shimizu, E.H. Hauri, G.D. Layne, Science 282 (1998) 1481.
[3] B.J. Fryer, S.E. Jackson, H.P. Longerich, Chem. Geol. 109 (1993) 1.
[4] I. Horn, R.L. Rudnick, W.F. McDonough, Chem. Geol. 164 (2000) 281.
[5] X.-H. Li, X. Liang, M. Sun, H. Guan, J.G. Malpas, Chem. Geol. 175 (2001) 209.
[6] N. Machado, A. Simonetti, in: P. Sylvester (Ed.), Laser-Ablation-ICPMS in the Earth Sciences, Min. Ass. Canada Short Course Series 29, 2001, 121.

[7] S.E. Jackson, N.J. Pearson, W.L. Griffin, in: P. Sylvester (Ed.), Laser-Ablation-ICPMS in the Earth Sciences, Min. Ass. Canada Short Course Series 29, 2001, p. 105.
[8] M. Tiepolo, Chem. Geol. 199 (2003) 159.
[9] K.P. Jochum, D.B. Dingwell, A. Rocholl, B. Stoll, A.W. Hofmann, S. Becker, A. Besmehn, D. Bessette, H.-J. Dietze, P. Dulski, J. Erzinger, E. Hellebrand, P. Hoppe, I. Horn, K. Janssens, G.A. Jenner, M. Klein, W.F. McDonough, M. Maetz, K. Mezger, C. Münker, I.K. Nikogosian, C. Pickhardt, I. Raczek, D. Rhede, H.M. Seufert, S.G. Simakin, A.V. Sobolev, B. Spettel, S. Straub, L. Vincze, A. Wallianos, G. Weckwerth, S. Weyer, D. Wolf, M. Zimmer, Geostandards Newslett. 24 (2000) 87.
[10] K.P. Jochum et al., in preparation.
[11] I. Raczek, K.P. Jochum, A.W. Hofmann, Geostandards Newslett. 27 (2003) 173.
[12] M. Rosner, A. Meixner, Geoanalysis (2003) 84 (abstract).
[13] K.P. Jochum, B. Stoll, A.W. Hofmann, I. Raczek, J. Pfänder, A. Meixner, M. Rosner, T. Vennemann, D.M.G. der Berichte, Beih. z. Eur. J. Miner. 14 (2002) 76.
[14] S. Gao, X. Liu, H. Yuan, B. Hattendorf, D. Günther, L. Chen, S. Hu, Geostandards Newslett. 26 (2002) 181.
[15] S. Eggins, Geostandards Newslett. 27 (2003) 147.
[16] M. Willbold, K.P. Jochum, Geostandards Geoanal. Res. (2004).
[17] N.J.G. Pearce, W.T. Perkins, J.A. Westgate, M.P. Gorton, S.E. Jackson, C.R. Neal, S.P. Chenery, Geostandards Newslett. 21 (1997) 115.
[18] J.D. Woodhead, J.M. Hergt, Geostandards Newslett. 25 (2001) 261.
[19] J.S. Fedorowich, J.P. Richards, J.C. Jain, R. Kerrich, J. Fan, Chem. Geol. 106 (1993) 229.
[20] M. Amini, Geochemistry of Fresh Submarine Glasses from the Hawaii Scientific Drilling Project-2, Diplomarbeit, Universität Mainz, 2003.
[21] K.J.R. Rosman, P.D.P. Taylor, Pure Appl. Chem. 70 (1998) 217.
[22] J.D. Woodhead, J.M. Hergt, Geostandards Newslett. 24 (2000) 33.
[23] J. Eisele, W. Abouchami, S.J.G. Galer, A.W. Hofmann, Geochem. Geophys. Geosyst. 4 (2003) 5.
[24] S.J.G. Galer, Chem. Geol. 157 (1999) 255.
[25] K. Govindaraju, Geostandards Newslett. 18 (1994) 1.
[26] J. Baker, D. Peate, T. Waight, C. Meyzen, Chem. Geol. 211 (2004) 275.